

Lawrence Berkeley National Laboratory

Recent Work

Title

The Martensitic Transformation in Silicon II. Crystallographic Analysis

Permalink

<https://escholarship.org/uc/item/2j2301wr>

Journal

Acta metallurgica materialia, 38(2)

Authors

Dahmen, U.
Westmacott, K.H.
Pirouz, P.
[et al.](#)

Publication Date

2017-12-05



Lawrence Berkeley Laboratory

UNIVERSITY OF CALIFORNIA

Materials & Chemical Sciences Division

National Center for Electron Microscopy

RECEIVED
LAWRENCE
BERKELEY LABORATORY

Submitted to Acta Metallurgica

JUL 12 1989

The Martensitic Transformation in Silicon II. Crystallographic Analysis

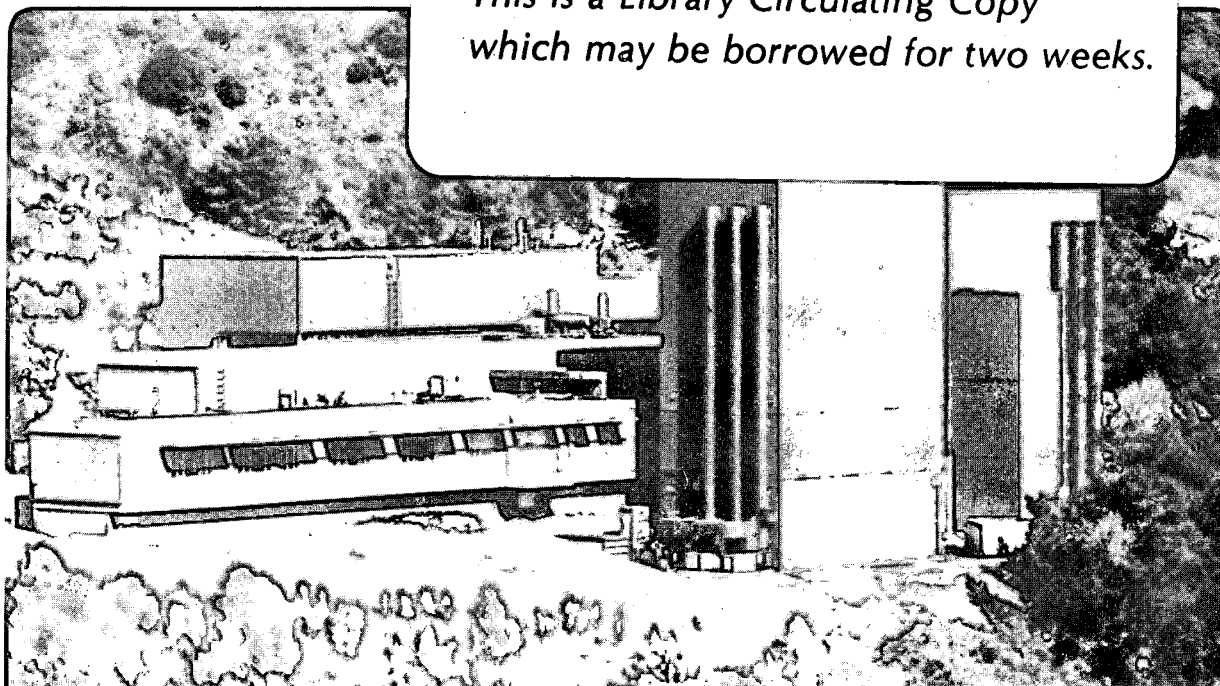
LIBRARY AND
DOCUMENTS SECTION

U. Dahmen, K.H. Westmacott, P. Pirouz, and R. Chaim

April 1989

TWO-WEEK LOAN COPY

*This is a Library Circulating Copy
which may be borrowed for two weeks.*



LBL-27072
e.2

DISCLAIMER

This document was prepared as an account of work sponsored by the United States Government. While this document is believed to contain correct information, neither the United States Government nor any agency thereof, nor the Regents of the University of California, nor any of their employees, makes any warranty, express or implied, or assumes any legal responsibility for the accuracy, completeness, or usefulness of any information, apparatus, product, or process disclosed, or represents that its use would not infringe privately owned rights. Reference herein to any specific commercial product, process, or service by its trade name, trademark, manufacturer, or otherwise, does not necessarily constitute or imply its endorsement, recommendation, or favoring by the United States Government or any agency thereof, or the Regents of the University of California. The views and opinions of authors expressed herein do not necessarily state or reflect those of the United States Government or any agency thereof or the Regents of the University of California.

**The Martensitic Transformation in Silicon
II. Crystallographic Analysis**

U. Dahmen and K.H. Westmacott

**National Center for Electron Microscopy
Materials and Chemical Sciences Division
Lawrence Berkeley Laboratory
1 Cyclotron Road
Berkeley, California 94720**

P. Pirouz and R. Chaim

**Department of Materials Science and Engineering
Case Western Reserve University
Cleveland, Ohio 44106**

April 1989

The Martensitic Transformation in Silicon

II) Crystallographic Analysis

U. Dahmen¹, K. H. Westmacott¹, P. Pirouz², and R. Chaim^{2*}

¹National Center for Electron Microscopy, Lawrence Berkeley Laboratory, University of California, Berkeley, CA 94720.

²Department of Materials Science and Engineering, Case Western Reserve University, Cleveland, OH 44106.

ABSTRACT

Following the experimental observations of the cubic→hexagonal transformation in silicon [1], a crystallographic analysis is presented in this paper. It is shown that the transformation is a more general mechanism of accommodating the local strain that is produced when twins in materials with a face centered cubic (fcc), or diamond cubic (dc), structure intersect. The same crystallography describes the propagation of a secondary twinning shear into its parent crystal, leading to a hexagonal plate on a {511} plane. The habit plane and orientation relationship predicted by this model are in exact agreement with observations by high resolution electron microscopy and diffraction of hexagonal platelets in hot-indented silicon reported in part I [1]. This agreement suggests that the transformation originates in deformation twinning and may be considered alternatively as a stress-induced martensitic transformation, or a lattice-variant accommodation shear.

1. INTRODUCTION

Cubic to hexagonal transformations are commonly found in fcc materials that exhibit polymorphism such as cobalt and its alloys. The reverse transformation is also observed in compound semiconductors with the wurtzite structure, e.g. CdS, SiC, etc. [2]. In all these materials, both the cubic and hexagonal forms are close-packed and differ only in the stacking sequence of the close-packed planes. Nearest-neighbor bonds remain identical and one structure may be regarded as a regularly faulted version of the other. A stacking fault on every other close-packed plane of the cubic lattice will transform the cubic ...ABCABC... stacking to the hexagonal ...ABABAB... stacking

and vice versa.

If the stacking fault energy is low, both forms are of comparable energy. Dislocations in such materials are therefore usually dissociated and stacking faults are commonly observed. Periodic arrangements of stacking faults other than on every second close-packed plane of the cubic lattice, polytypes, have been observed in many materials, most notably SiC where polytypes with repeat distances of more than 100 close-packed planes have been found. The Ramsdell notation [3] describes these according to repeat distance and rhombohedral (R) or hexagonal (H) symmetry; e.g. the hcp structure is denoted 2H.

The orientation relationship between the different polytypes, e.g. the cubic and hexagonal phase, is always simple: close-packed planes and close-packed directions remain parallel. The plane of contact, or habit plane, is the close-packed plane.

In sharp contrast, the orientation and habit plane relationship of the diamond hexagonal (dh) phase observed in silicon are unusually complex, and reminiscent of martensitic transformations [1].

2. RESULTS

It has been shown that twinning is the major mode of deformation in the indentation of Si at intermediate temperatures [4-6]. Unlike dislocations which can glide in either direction, normal twinning can shear a crystal only in one direction and not its reverse. This polarization leads to some interesting interactions between twins and it is believed to be ultimately responsible for the occurrence of the hexagonal phase.

2.1. Hexagonal Phase at Twin Intersections

Intersecting twins in fcc alloys have been studied in detail by Blewitt et al. [7] and more recently by Mahajan and co-workers [8-10], and to simplify the problem we will initially treat an fcc lattice as well; extension to the dc structure is then relatively straightforward.

Consider the twinning sequence depicted in a $\langle 110 \rangle$ projection in Fig. 1. A first twin band is formed by passing Shockley partial dislocations across successive close-packed planes resulting in a homogeneous simple shear transformation T_1 of magnitude $\gamma = (1/2)^{1/2}$ on a $\{111\}$ shear plane (Fig. 1a). The shape change is visible as a kink in the crystal and can be measured as surface relief where a twin band intersects the surface. When a second twin band crosses the first, the region of inter-

section undergoes a homogeneous transformation that is the product of the two complementary twinning shears T_1 and T_2 :

$$P = T_2 T_1$$

From the schematic in Fig. 1b, it can be seen that this is not a twinning shear and does in fact change the lattice. Further examination of Fig. 1b shows that the lattice in the region of intersection is related to that of twin 2 by a simple shear on the common close-packed planes in the reverse direction of a twinning shear. A rigorous proof for this is given in the appendix. The effect of such a shear on the atomic arrangement is shown in Fig. 2 where a normal (forward) twinning shear (Fig. 2a) is compared to its reverse (Fig. 2b). By passing a $+1/6 \langle 112 \rangle$ Shockley partial dislocation across every $\{111\}$ plane, the ...ABCABC... stacking of the matrix is changed to the ...CBACBA... stacking of the twin. Fig. 2b illustrates that the reverse, passing a $-1/6 \langle 112 \rangle$ partial across every $\{111\}$ plane, changes the ...ABCABC... stacking of close-packed planes in the matrix to a highly unfavorable ...AAAAAA... stacking sequence. However, an energetically favorable configuration is obtained if, as shown in Fig. 2c, atomic shuffles on every other plane change the ...AAAAAA... stacking to the ...ABABAB... sequence of the hexagonal lattice. This is the equivalent of passing a $-1/3 \langle 112 \rangle$ dislocation across every other close-packed plane rather than $-1/6 \langle 112 \rangle$ dislocation across every plane.

The more usual mode of fcc to hexagonal transformation, shown in Fig. 2d, produces the same structural change by half the shear in the opposite direction, i.e. a $+1/6 \langle 112 \rangle$ dislocation, instead of $-1/3 \langle 112 \rangle$, on every other close-packed plane. It is interesting to note that this is entirely equivalent to the well-known alternatives in twinning [11]: just as a twin can be produced by passing either a $+1/6 \langle 112 \rangle$ or a $-1/3 \langle 112 \rangle$ partial across every close-packed plane, the hexagonal phase can be formed by passing the same two partials across every other plane. Measurements of surface relief have shown that usually the alternative with the smaller shear angle operates [11,9]. However, as shown above and in the appendix, at the intersection of two twins, compatibility requirements dictate the high angle shear.

From these considerations it is clear that the region of intersection undergoes a homogeneous shear with additional shuffles leading to hexagonal material with close-packed planes parallel to its interface with the crossing twin (twin 2). With respect to the crossed twin (twin 1) the hexagonal region has a $\{511\}$ habit plane. This habit and orientation relationship are identical to

the observed crystallography of hexagonal plates in Si, but unlike the observed structures, the hexagonal region is confined to the twin intersection. This apparent discrepancy is resolved by considering a different sequence of events. However, it should be mentioned that the formation of hexagonal phase at the intersection of twins, as shown in Fig. 1b, has been confirmed recently [12].

2.2. Hexagonal Phase from Secondary Twinning

If the role of the matrix and twin 1 are interchanged, then twin 2 becomes a secondary twin (i.e. a twin of a twin) with respect to the matrix. Thus if local stress conditions lead to a secondary twin being nucleated within the first twin, its propagation into the matrix would lead to development of a hexagonal {511} plate (see Fig. 1c). The observed crystallography can therefore be understood simply in terms of the propagation of secondary twins into the matrix.

Deformation twinning may be considered a martensitic transformation in which the martensite structure happens to be a mirror image of the parent structure. In a similar manner, the {511} hexagonal plates may be considered a martensitic transformation. Fig. 1b shows that the transformation strain P is a simple shear of magnitude $\gamma = (1/2)^{1/2}$, the same as a twinning shear on a high-index {511} plane. The $1/6 \langle 112 \rangle$ twinning dislocations in the secondary twin become $1/18 \langle 255 \rangle$ dislocations in the matrix [10], but the spacing and packing density of the {511} planes in the matrix differ by a factor of three from that of the {111} planes in the secondary twin. Thus a growth mechanism based on the direct propagation of individual twinning dislocations from the secondary twin into the matrix would require further dissociation of the twinning dislocations into three $1/64 \langle 255 \rangle$ partials -- a procedure of dubious physical significance. The atomic displacements during this shear are indicated in a close-up view in Fig. 3a. Notice that these lead to a structural change identical to the previous description of a reverse twinning shear relative to the secondary twin and thus leaves the problem of ...AAAAAA... stacking to be resolved.

2.3. Coincidence Site Lattice

It is well-known that one of the simplest coincidence site lattices (CSL), the $\Sigma 3$ CSL is the lattice common to two twin-related fcc crystals. Fig. 3b shows the two $\Sigma 3$ CSLs associated with the two intersecting twin boundaries in Fig. 3a. These two CSLs may themselves be considered to be twin-related and form another CSL, the $\Sigma 9$ CSL also illustrated in Fig. 3b. Note that the hexagonal

phase, being related to both twins, shares the $\Sigma 9$ CSL. To clarify this complex figure, the four different coincidence site lattices, $\Sigma 1$, $\Sigma 3$, $\Sigma 3$ and $\Sigma 9$ are shown separately at reduced size below Fig. 3b. It can be seen that the $\{511\}$ interface is a low-index plane in the $\Sigma 9$ CSL (shaded) and the repeat unit along this interface is six close-packed plane spacings. If any faulting were to occur in the hexagonal phase, it might be expected to leave the $\Sigma 9$ framework unaltered. In fact, some faulting is likely to occur because compatibility criteria prescribe the macroscopic deformation, or shape change, of a twin intersection, not the sequence of the accommodating dislocations. Any stacking order is allowed within the overall constraints that the accommodation strain must be the reverse twinning shear, ...AAAAAA... stacking is avoided, and the $\Sigma 9$ CSL is to be preserved. Electron diffraction has revealed that hexagonal Si plates do in fact show a propensity for faulting with an interesting tendency to confine faults to one of the two hcp sublattices [1].

2.4. Extension to the dc Lattice

The foregoing presentation of the crystallography was given in terms of fcc lattices, but the same reasoning applies to dc lattices. The $\{511\}$ habit plane of the hexagonal phase then becomes identical to the model given by Tan et al. [13], or by Moller [14], based on five- and seven-membered rings. The absence of dangling bonds shows that this is indeed a coherent interface. Fig. 4 is a schematic of the interface shown in previous figures for fcc lattices, completed for dc lattices.

2.5. Interaction of Hexagonal Phase and Twins

In the heavily deformed regions of the Si near the indentations, the high density of propagating twins and hexagonal plates leads to a variety of mutual interactions. This aspect has not been studied in detail but several examples may be found in the illustrations of paper I. Generally, twins and hexagonal bands are obstacles for other non-parallel twins and hexagonal bands. Thus, two twins will cross each other only if the local shear stress is sufficiently large. The amount of energy necessary to force an interaction will depend on the difficulty of strain accommodation as well as the relative width of the twin or hexagonal bands, i.e. a narrow band is easier to cross than a wide one, and a wide band crosses more easily than a narrow one. For two twins, it has been shown theoretically here and experimentally in Ref. 12 that this strain accommodation can be

accomplished by transformation to the hexagonal structure. Other, more energetically expensive accommodation modes are possible and have in fact been observed. For most intersections of hexagonal bands with twins or other hexagonal bands, no simple accommodation mode analogous to the $dc \rightarrow dh$ transformation is apparent. However, intersections are still possible, given sufficient shear stresses. Figs. 1 and 5 of paper I show regions where different interactions are occurring.

One special interaction should take place when a hexagonal band crosses a twin belonging to the same family as the one that originally gave rise to it. This is simply the reverse of the original formation of the hexagonal phase and will revert the lattice to cubic stacking in the region of intersection.

3. DISCUSSION

The intersection of a twin by slip dislocations or by another twin has been examined in detail by Mahajan and coworkers [8-10] using Co-Fe alloys deformed either in plane strain compression at ambient or by bending at liquid nitrogen temperature. These authors recognized that homogeneous shear would lead to AA stacking in the twin intersection and suggested multiple twinning as an accommodation mode. This is a form of strain accommodation often found in martensite plates. However, it locally violates the plane strain character of the deformation, and the alternative of hexagonal phase formation is equally consistent with the experimental results in Ref. [10].

By analogy with martensitic transformations, the strain accommodation of a secondary twin propagating into the matrix can be accomplished in a variety of ways. As shown in section 2, strain accommodation by homogeneous shear would lead to high energy AA stacking corresponding to a Shockley partial dislocation on every close packed plane. However, several other possibilities exist for distributing the strain in the interface. By shuffling alternate layers, the high energy associated with AA stacking can be reduced to that of a faulted or perfect hexagonal structure. This corresponds to two Shockley partial dislocations ($b = -1/3 \langle 112 \rangle$) on every other close packed plane. It is clear from the experimental results given in part I [1] that this is the structure that forms under the present deformation conditions. Other, less homogeneous, strain distributions, corresponding to other dislocation stacking sequences could arise under different deformation conditions. For example, combining three Shockley partials ($b = -1/2 \langle 112 \rangle$) on every third close packed plane would maintain the cubic structure of the secondary twin. This corresponds to strain

accommodation by perfect dislocations (lattice invariant shear) and the resulting interface structure is that of a $\Sigma 9$ grain boundary on a $\{511\}$ habit plane (see Fig. 3). Finally, it is also possible to accommodate the strain by the multiple twinning mechanism advanced by Mahajan and Chin [10]. Which particular mode of strain accommodation is most favorable would thus depend on the relative magnitudes of these strain and fault energy terms and could well be sensitively balanced.

Each of the modes of accommodation has its parallel in martensitic transformations. For example, martensite plates in Cu-Al exhibit polytype structure [15]; martensite laths in low-carbon steels show dislocation structures [16]; and martensites in In-Fe alloys are heavily twinned [17]. The similarities between the accommodation of secondary twins and martensitic transformations will be discussed in part III [18].

Appendix

It can be seen from Fig. 1c that secondary twinning amounts to a rotation relative to the matrix. This rotation can be accommodated by the reverse twinning shear of the secondary twin causing the transformation from cubic to hexagonal stacking. The primary twin (1) has two complementary twinning shears: T_2 which transforms it to the secondary twin (2), and T_1 which transforms it to the matrix (M). Its inverse T_1^{-1} transforms the primary twin to the matrix.

When expressed in terms of these two shears T_1 and T_2 the transformation between the different parts of the crystal in Figs. 3 and 1(c) can be written as follows:

$$\begin{aligned}
 1 \rightarrow 2 & : T_2 \\
 1 \rightarrow M & : T_1 \\
 M \rightarrow 1 & : T_1^{-1} \\
 M \rightarrow 2 & : T_2 T_1^{-1} \\
 2 \rightarrow H & : T_2 T_1 T_2^{-1}
 \end{aligned}$$

Thus the transformation $M \rightarrow H$ is given by $P = T_2 T_1 T_2^{-1} T_2 T_1^{-1} = T_2$. It is also apparent from Fig. 1c that the transformation $M \rightarrow H$ is the same as $1 \rightarrow 2$, i.e. $P = T_2$, but in its expanded form it is easier to separate the rotation and accommodation components.

First, it can be seen that secondary twinning, i.e. the transformation $M \rightarrow 1 \rightarrow 2$ is identical to a rigid body rotation, as follows: the two complementary twinning shears T_1 and T_2 are related to the same pure shear D by opposite rotations R and R^T :

$$\mathbf{T}_1 = \mathbf{R}^T \mathbf{D}$$

$$\mathbf{T}_2 = \mathbf{R} \mathbf{D}$$

Hence:

$$\mathbf{T}_2 \mathbf{T}_1^{-1} = \mathbf{R} \mathbf{D} \mathbf{D}^{-1} \mathbf{R} = \mathbf{R} \mathbf{R}$$

is a rigid body rotation through approximately the shear angle. This is true for any two complementary simple shears. For a twinning shear, the rotation of 39° between M and 2 is directly visible in Figs. 3 and 1c. That the accommodation shear $\mathbf{T}_2 \mathbf{T}_1 \mathbf{T}_2^{-1}$ is in fact the reverse twinning shear of the secondary twin (twin 2) can be seen from the distortion of the unit parallelograms of the lattice in Fig. 1c. This can be proved more rigorously by first noting that:

$$\mathbf{T}_2 \mathbf{T}_1 \mathbf{T}_2^{-1} = \mathbf{T}_2 \mathbf{R}^T \mathbf{R} \mathbf{T}_2^{-1}$$

When expressed in terms of the two complementary shears of twin 2, denoted by italics:

$$T_1 = \mathbf{R} \mathbf{D}$$

and: $2 \rightarrow 1 : T_2 = \mathbf{R}^T \mathbf{D} = \mathbf{T}_2^{-1}$

This becomes:
$$\begin{aligned} \mathbf{T}_2 \mathbf{T}_1 \mathbf{T}_2^{-1} &= \mathbf{D}^{-1} \mathbf{R} \mathbf{R}^T \mathbf{R} \mathbf{T}_2^{-1} \\ &= T_1^{-1} \end{aligned}$$

The similarity with the basic equation of martensite theory now is apparent:

$$\mathbf{P} = T_1^{-1} \mathbf{R} \mathbf{R}$$

a lattice-invariant "transformation" $\mathbf{R} \mathbf{R}$ is accommodated by a lattice-variant shear T_1^{-1} to form an invariant plane strain $\mathbf{P} = \mathbf{T}_2$. The interesting difference to conventional martensitic transformations is the fact that the new phase is thermodynamically stable only under the specific conditions of stress imposed by the deformation. It serves to accommodate, rather than be accommodated by, the deformation.

ACKNOWLEDGEMENT

U. D. and K. H. W. acknowledge the support of their work by the Director, Office of Energy Research, Office of Energy Sciences, Materials Sciences Division of the U.S. Department of Energy under contract DE-AC03-76SF00098.

* Present address: Department of Materials Engineering, Technion, Haifa, 32000 Israel.

REFERENCES

1. P. Pirouz, R. Chaim, U. Dahmen, and K. H. Westmacott, Submitted to *Acta Metall.* (1989).
2. P. Pirouz, *Scripta Met.* **23**, 401 (1989).
3. L. S. Ramsdell, *Am. Mineral.* **32**, 64 (1947).
4. V. G. Eremenko and V. I. Nikitenko, *Phys. Stat. Sol (a)* **14**, 317 (1972).
5. K. Yasutake, J. D. Stephenson, M. Umeno, and H. Kawabe, *Phil. Mag. A* **53**, L41 (1986).
6. P. Pirouz, *Scripta Met.* **21**, 1463 (1987).
7. T. H. Blewitt, J. K. Redman, F. A. Sherrill, and R. R. Coltman, *Phys. Rev.* **98**, 1555 (1955).
8. S. Mahajan and G. Y. Chin, *Acta Met.* **21**, 173 (1973).
9. S. Mahajan and D. F. Williams, *Int. Metallurg. Rev.* **18**, 43 (1973).
10. S. Mahajan and G. Y. Chin, *Acta Met.* **22**, 1113 (1974).
11. A. Kelly and G. W. Groves, "Crystallography and Crystal Defects". London: Addison-Wesley, (1970).
12. U. Dahmen, C. Hetherington, P. Pirouz, and K. H. Westmacott, *Scripta Met.* **23**, 269 (1989).
13. T. Y. Tan, H. Foll, and S. M. Hu, *Phil. Mag. A* **44**, 127 (1981).
14. P. Pirouz, J. Yang, F. Ernst, and H.-J. Moller, *Mat. Res. Soc. Symp. Proc.* **139**, (1988). In press.
15. T. Saburi and C. M. Wayman, *Acta Metall.* **27**, 979 (1979).
16. K. Wakasa and C. M. Wayman, *Metallography* **14**, 49 (1981).
17. Z. S. Basinski and J. W. Christian, *Acta Metall.* **2**, 148 (1954).
18. P. Pirouz, U. Dahmen, K. H. Westmacott, and R. Chaim, Submitted to *Acta Metall.* (1989).

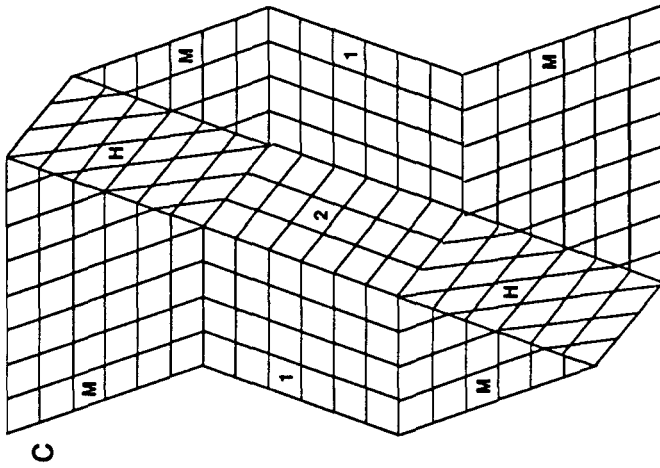
Figure Captions

Fig. 1 Schematic illustration of twinning sequences where M denotes the matrix, 1 and 2 are twins and H is hexagonal phase. A single twin band is shown in (a); in (b) the first twin is crossed by a second twin band causing the intersection region to undergo a reverse twinning shear as seen from the distortion of the unit parallelogram of the lattice; in (c) the same distortion is caused by a secondary twinning shear propagating into the matrix.

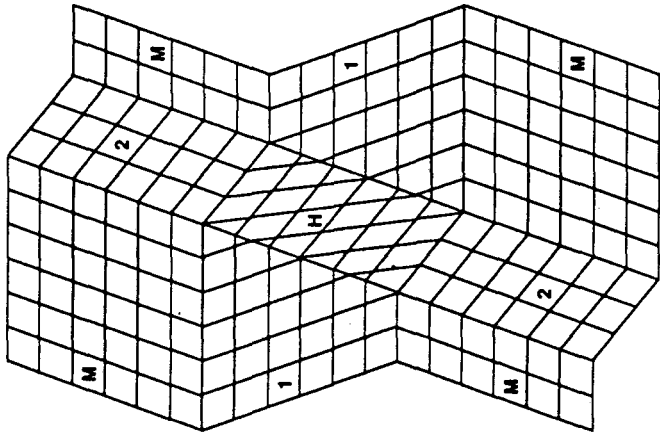
Fig. 2 $\langle 110 \rangle$ projection of fcc lattice with atoms at different heights shown as open and solid circles. (a) shows forward twinning shear and (b) its reverse leading to unfavorable AA stacking which is shuffled to hexagonal ...ABABAB... stacking in (c); the same hexagonal ...ABABAB... stacking can be achieved by half the twinning shear in the forward direction as seen in (d).

Fig. 3 Close-up view of fcc matrix (M) in $\langle 110 \rangle$ projection with primary (1) and secondary (2) twins and transformed region (H). In (a) atomic displacements during homogeneous shear on $\{511\}$ habit plane (shaded) resulting in AA stacking are indicated by arrows; shuffles are added in (b) to provide hexagonal ...ABABAB... stacking; (b) also illustrates coincidence site lattices: the two $\Sigma 3$ CSLs for the two twins and their common $\Sigma 9$ CSL are indicated by solid lines. A separate rendition of the CSLs in reduced size is shown in the four lattices below the main figure, illustrating $\Sigma 1$, two different $\Sigma 3$ and their common $\Sigma 9$ CSL.

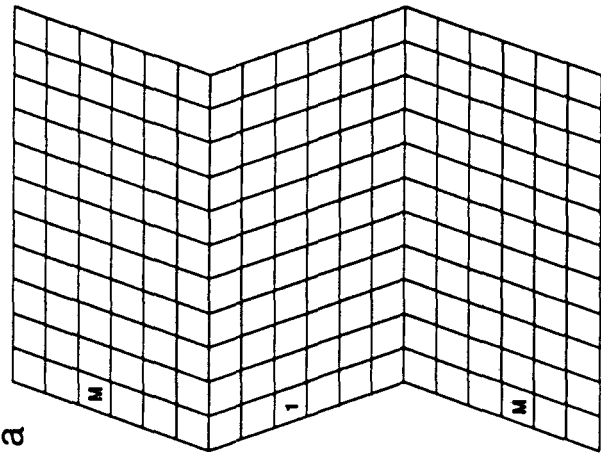
Fig. 4 Magnified view of $\{511\}$ hexagonal phase showing atom positions of diamond cubic lattice. The cubic/hexagonal interface is coherent with alternating five- and seven-membered rings, identical to the model of Tan et al. [13]. The fcc lattice shown lightly in the background is a section of Fig. 1b and 1c.



XBL 894-1311

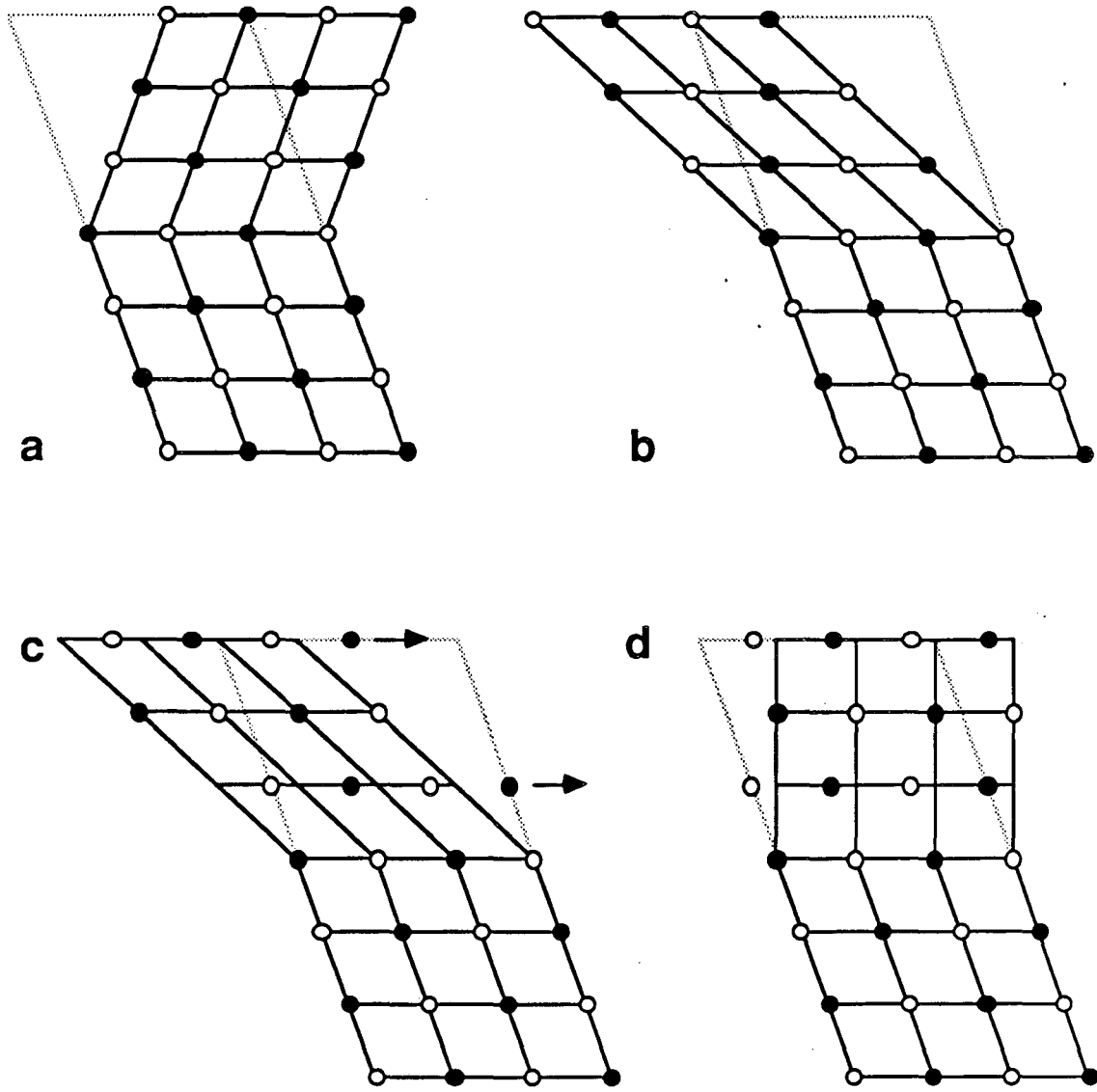


b



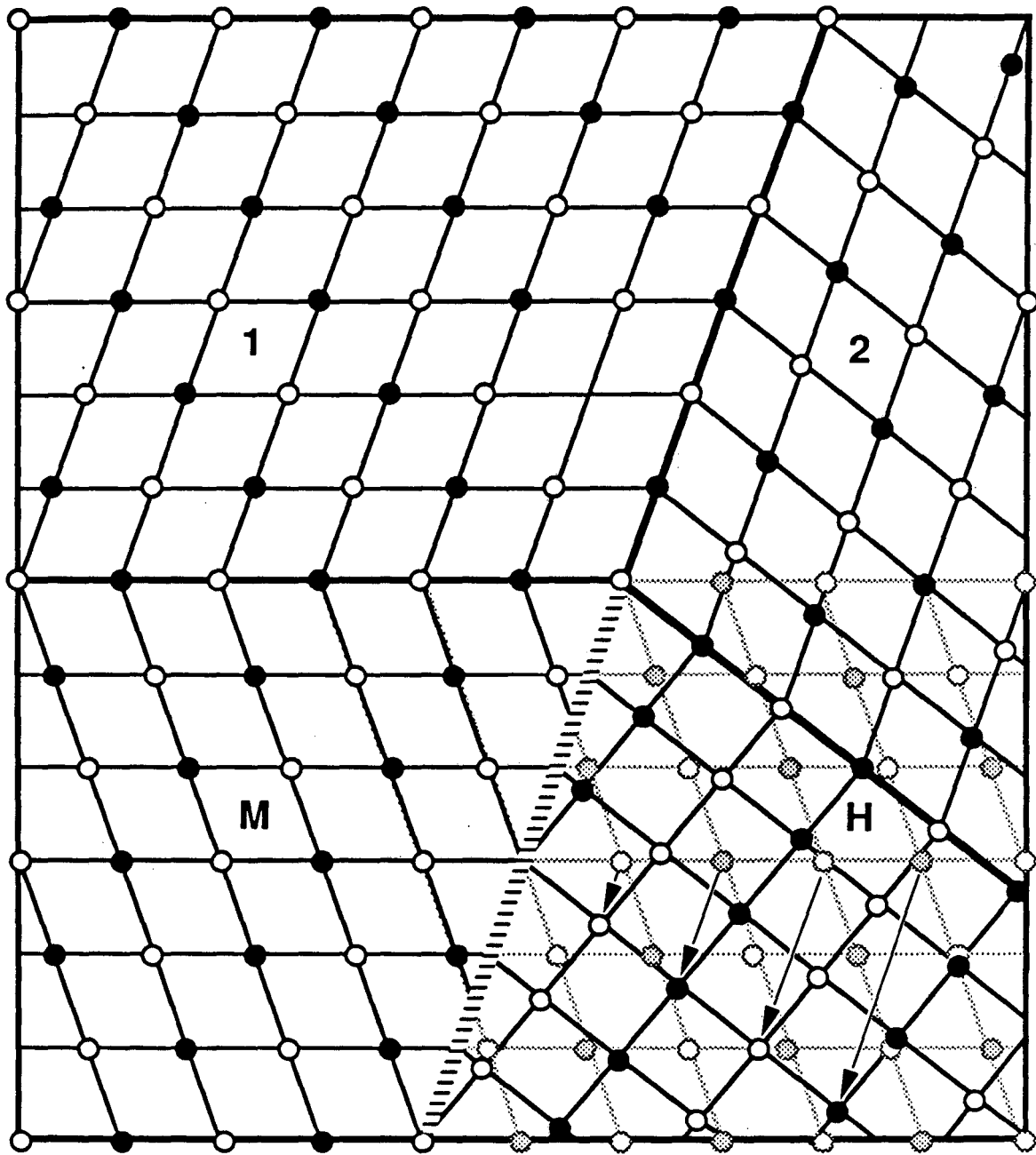
a

Figure 1



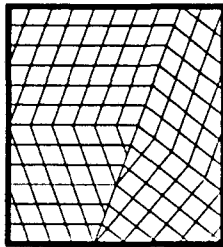
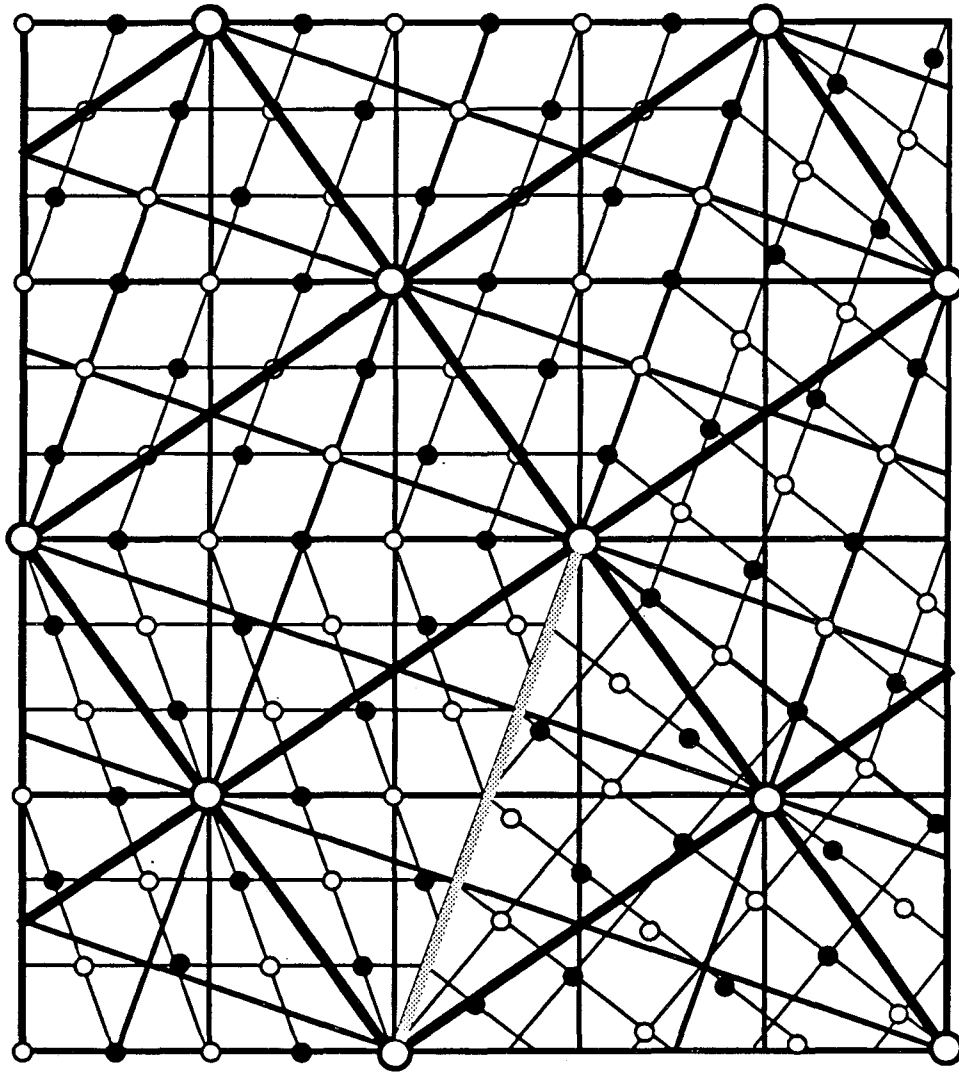
XBL 894-1312

Figure 2

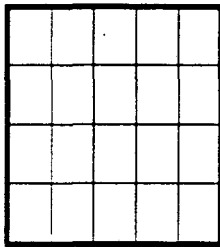


XBL 894-1313

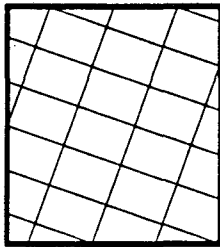
Figure 3a



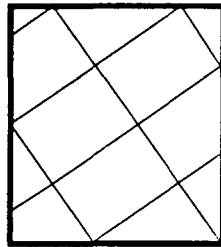
$\Sigma 1$



$\Sigma 3$



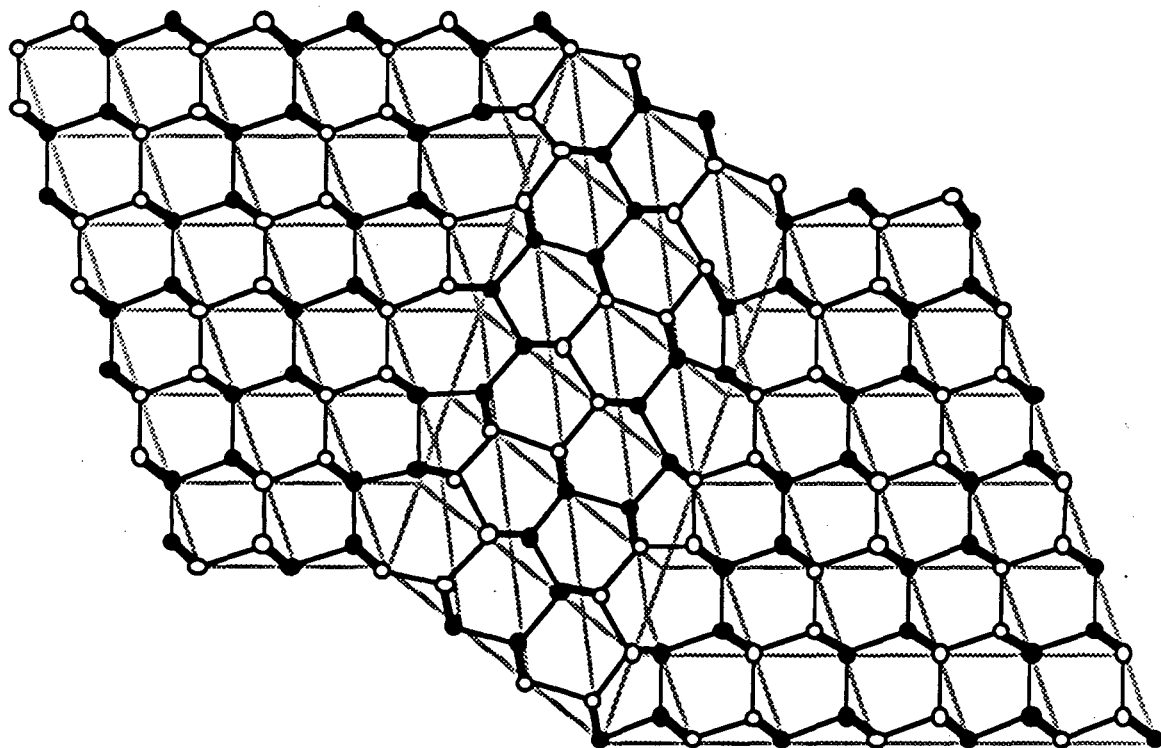
$\Sigma 3$



$\Sigma 9$

XBL 894-1314

Figure 3b



XBL 894-1315

Figure 4

LAWRENCE BERKELEY LABORATORY
TECHNICAL INFORMATION DEPARTMENT
1 CYCLOTRON ROAD
BERKELEY, CALIFORNIA 94720